Investigations of the breakdown transition, hysteresis, and periodic-pulse oscillation in Tl/W-doped blue bronzes

Mingliang Tian and Zhiqiang Mao
Structure Research Laboratory, University of Science and Technology of China, Academia Sinica, Hefei 230026, People's Republic of China

Yuheng Zhang
Structure Research Laboratory, University of Science and Technology of China, Academia Sinica, Hefei 230026, People's Republic of China
and Chinese Center of Advanced Science and Technology, World Laboratory, P.O. Box 8730, Beijing 100080, People's Republic of China

Jing Shi
Department of Physics, Wuhan University, Wuhan 430072, China

Decheng Tian
Department of Physics, Wuhan University, Wuhan 430072, China
and International Center of Material Physics, Academia Sinica, Shenyang 110015, People's Republic of China
(Received 27 April 1993; revised manuscript received 30 August 1993)

Nonlinear transport behavior, which shows a sudden breakdown transition to zero- or negative-differential resistance in the high field, is observed in the quenched thallium- or tungsten-doped blue bronzes $K_{0.15}Tl_{0.15}MoO_3$ and $Tl_{0.3}Mo_{1-x}W_xO_3$ at 77 K. It is found that the critical breakdown transition threshold is unstable for the induced field and decreases with increasing cycling times of the conducting current and, finally, reaches a definite value. When the current increases from 30 to 100 mA, the voltage between the two ends of the sample does not show a clear increase, i.e., a similar phenomenon with zero-differential resistance. On the downward cycle of the current, the voltage-current curve exhibits a large electronic hysteresis over the nonlinear region. On the other hand, in the critical region, the breakdown transition is usually accompanied by a voltage pulse with a large amplitude and exhibits a negative-differential resistance. These effects of an electric field on a pinned charge-density wave are phenomenologically interpreted in analogy with the mechanical deformations of the crystal solid.

I. INTRODUCTION

Potassium blue bronze $K_{0.3}MoO_3$ has a quasi-one-dimensional electronic structure[1] and undergoes a Peierls transition around 180 K.[2] Since Dumas *et al.*[3] found nonlinear conductivity resulting from the sliding motion of a charge-density wave (CDW) in the presence of an electric field, much effort has been devoted to the study of this material in order to investigate a rich variety of nonlinear electronic transport phenomena.[4–9] Recently, it has been noted that at low temperatures (about $T<40$ K) in pure $K_{0.3}MoO_3$ an abrupt transition from an insulating to a highly conducting state can be induced by an electric field,[10–16] and this phenomenon has often been compared to the model of Fröhlich "sliding-mode" conductivity, which was an early attempt to explain superconductivity.[17] While the field exceeds a definite threshold field E_T (typically 100 V/cm), the measured dV/dI shows a sudden decrease, and a very large noise of typically a few millivolts is associated with the sudden decrease of dV/dI. Current densities up to 10^4 A cm^{-2} and a dynamic resistivity less than 10^{-4} cm^{-2} can be achieved.[12] These unusually sharp nonlinear characteristics were considered to be a qualitative change in charge-density-wave dynamics as normal carriers freeze out.[10,12,16] It has been speculated that the transition represents a rigid motion of the highly coherent CDW in the manner of the original Fröhlich mode.

Up to now, the so-called "breakdown" phenomena in $K_{0.3}MoO_3$ were all found in low temperatures. Above 40 K, no similar phenomena were reported. The reason for this generally was considered to be due to at least two important aspects. The first is the notion of pinning by impurities which moves the Fröhlich mode from zero to a finite frequency.[18] The second is the viscous damping of CDW motion by normal-carrier screening.[19,20] The results of these assumptions are that a CDW motion above a threshold field is characterized by deformations and backflow currents of charge carriers thermally excited across the Peierls gap at high temperature.

In this paper, we report a similar breakdown phenomenon at 77 K from a damping state to a near-zero-differential resistance state in Tl-doped $K_{0.15}Tl_{0.15}MoO_3$ and W-doped $Tl_{0.3}Mo_{1-x}W_xO_3$ ($x<0.1$) blue bronzes. We found that the second threshold field of transition is unstable for the induced field, and in the transition region a large hysteresis and periodic low-frequency voltage pulse oscillation with large amplitude were also clearly observed.

II. EXPERIMENTAL PREPARATIONS

Single crystals of pure and Tl/W-doped blue bronzes used in this study were prepared by electrolytic reduction method with a definite molar ratio of K_2CO_3-MoO_3, K_2CO_3-Tl_2CO_3-MoO_3, and Tl_2CO_3-MoO_3-WO_3 melt, respectively. The resulting crystals were characterized by the electron-probe, x-ray diffraction method. The unit cell parameters of three samples are, respectively, $a=18.245$, 18.331, and 18.464 Å, $b=7.540$, 7.542, and 7.543 Å, $c=9.850$, 9.931, and 10.014 Å, $\beta=117.65$, 118.36, and 118.39. The required powder materials of growing crystals mentioned above are different from the traditional ones with A_2MoO_4-MoO_3 or A_2MoO_4-MoO_2-MoO_3 (A=K,Tl) mixture. Transport and thermopower measurements[21] show a metal-semiconductor transition at about 180, 161, and 170 K, respectively, for the three samples. A Raman-scattering[22] study also found a partially softening CDW amplitude mode at about 57 cm^{-1} for pure and Tl-doped samples in the distorted state. These results are consistent with that grown by using A_2MoO_3-MoO_3 (A=K,Tl) melt. All measurements of samples $K_{0.3}MoO_3$, $K_{0.15}Tl_{0.15}MoO_3$, and $Tl_{0.3}Mo_{1-x}W_xO_3$ ($x<0.1$) were performed by a two-probe method in a constant-current mode. The sample was immersed in liquid nitrogen to avoid the Joule-heating effect in high current conditions. Electrical contacts were made by soldered indium on the evaporated Au film and confirmed that the magnitude of the contact resistance was smaller than that of the sample itself. The results presented here were obtained on the pure, Tl-doped, and W-doped samples with dimensions of about $3\times1.5\times0.5$, $3.5\times1\times0.1$, and $2\times1\times0.1$ mm^3, respectively. The dc voltage-current (V-I) characteristics were recorded by an X-Y recorder under a sweeping dc.

III. RESULTS

Figure 1 shows the voltage-current (V-I) characteristics measured in $K_{0.15}Tl_{0.15}MoO_3$ with the dc mode at 77 K. It is seen that in the initial measurements for the virgin sample quenched by liquid nitrogen, the V-I characteristics present normal viscous damping transport behavior without a breakdown transition in high field, as shown in Fig. 1(a). The critical region of the threshold is smooth, the magnitude of the threshold field is about 1.8 V/cm. In this viscous damping state of charge-density waves, no large hysteresis in the nonlinear transport region is found. However, when the sample has continually undergone many cycles of the high conducting current repeatedly, the V-I characteristic curve suddenly presents an onset of a voltage drop by about 50% at about 75 mA, and, clearly, gives a second threshold I_{T2} in the high field. Such a switching behavior is unstable for the induced field, and in subsequent measurements, the magnitude of the threshold voltage decreases with the increase of the cycling times of the driven current as shown in Fig. 1(b).

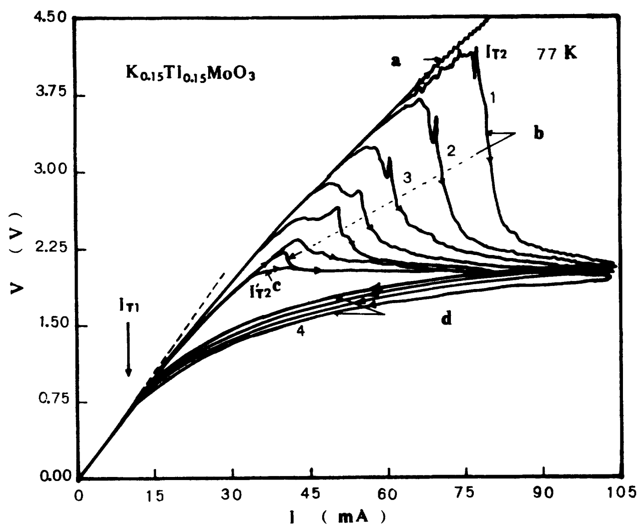

FIG. 1. Voltage-current (V-I) characteristics measured in $K_{0.15}Tl_{0.15}MoO_3$ with dc mode at 77 K. (a) is one of the typical normal V-I curves without breakdown transition recorded in the virgin sample quenched by liquid nitrogen. After many high conducting current cycles were applied repeatedly to the sample, an abrupt breakdown-transition behavior occurred. For the subsequent current cycles, the corresponding series of curves are shown in (b); the interval of the waited time of the two neighboring curves measured is about 3 min, the sweeping rate of current is about 1 mA/s. c is the final steady V-I characteristic with zero-differential resistance. The four curves labeled (d) are the downward cycle curves of the curves 1–3 and (c), respectively.

When the sample is repeatedly electronically cycled by the high conducting current for about 30 min, the system gradually reaches a steady conducting state with near-zero-differential resistance above the second threshold I'_{T2} as shown in Fig. 1(c), the current increases from 30 to 100 mA, the voltage of the two ends of the sample does not show an observable increase, i.e., $dV/dI\sim0$. In this final state, when the current decreases from 100 to 0 mA, a large hysteresis in the nonlinear transport region occurs, as shown in Fig. 1(d-4). The three other downward cycle curves correspond to those of Figs. 1(b-1), 1(b-2), and 1(b-3), respectively. In addition, in the critical region of the second threshold transition of Fig. 1(b), the abrupt breakdown transition is not infinitely sharp, instead it has a finite negative slope accompanied by a sharp voltage pulse near the leading edge above the critical point I_{T2}. This onset point I_{T2} is changed for different quenching times by liquid nitrogen. In this paper we only show one of the results. If the sample with near-zero-differential resistance shown in Fig. 1(c) is switched off the conducting current and kept at 77 K for about 1 h or longer, only the similar phenomena with a voltage drop at the critical point can be partially recovered again, but the normal form of the V-I curve with a smooth threshold point shown in Fig. 1(a) does not appear, unless the sample is quenched again by (LN_2), as shown in Fig. 2. In this case the amplitude of the voltage drop at the critical point I_{T2}

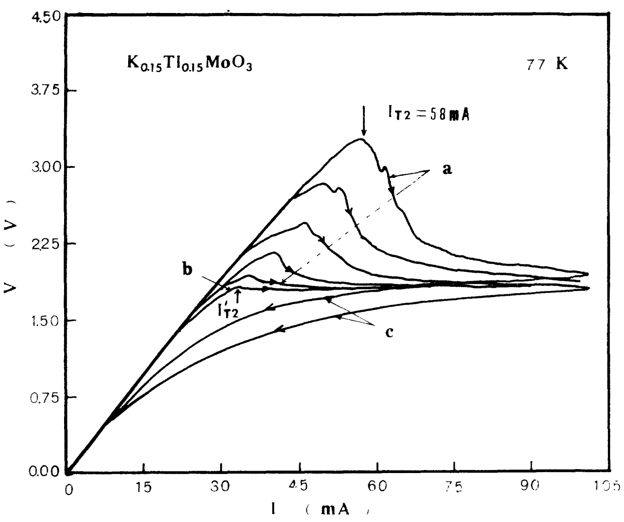

FIG. 2. After the sample with a steady zero-differential resistance state is switched off the conducting current and kept at 77 K for 3 h, we again obtained the corresponding voltage-current characteristics of $K_{0.15}Tl_{0.15}MoO_3$

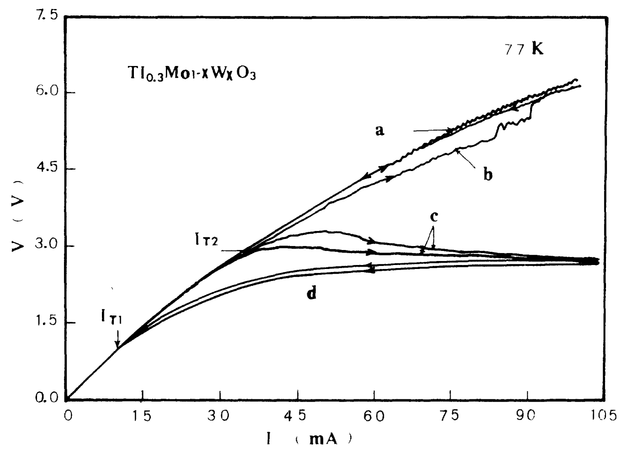

FIG. 3. Voltage-current (*V-I*) characteristics for the W-doped sample $Tl_{0.3}Mo_{1-x}W_xO_3$ ($x<0.1$) at 77 K. (a) is the typical normal *V-I* curve without breakdown transition, similar to Fig. 1(a), (b) is the usually *V-I* curve derived from (a), but not a breakdown transition after the sample has experienced a series of high conducting current cycles. The two curves in (c) are the curves with a near-negative-differential resistance, (d) is the downward cycle curve of (c).

is less than that shown in Fig. 1(b), and the second critical transition also becomes rather smooth and presents a negative slope instead of the very sharp feature in Fig. 1(b). If the sample is continually kept in the high field, the CDW system will still remain in its zero-differential resistance state. Therefore, the so-called final steady state actually is a quasisteady state under the repeated high conducting current cycling. These phenomena mentioned above are reproducible for the repeated thermal cycling rising to room temperature. In a W-doped sample, we also observed a similar behavior with a negative- or zero-differential resistance accompanied by a large hysteresis under the conducting current cycles repeatedly as shown in Fig. 3, but we do not observe a corresponding large voltage drop at the critical point. The transit from the viscous damping *V-I* characteristics to that with a zero dV/dI form seems to be abrupt. In pure blue bronze $K_{0.3}MoO_3$ we did not observe a similar breakdown transition to the zero-differential resistance state in a high field at 77 K. In contrast, for a normal switching shown in Fig. 4, the switching and threshold are independent of the conducting current cycles; the hysteresis can only be observed near the second critical threshold region.

Figure 5 shows the low-frequency periodic-voltage pulse oscillation spectra of $K_{0.15}Tl_{0.15}MoO_3$ recorded by the *X-Y* recorder as a time function at the second critical point (b) of the curve in the inseted plot. The inseted plot is the typical *V-I* characteristics of the $K_{0.15}Tl_{0.15}MoO_3$ sample, curve (A) is a normal viscous damping transport form without a large voltage drop, which is similar to Fig. 1(a). The arrows labeled (a), (b), and (c), respectively, represent the second critical point I_{T2} to the presented abrupt voltage drop for the subsequent current cycles; the values of the threshold are about 77, 72, and 47 mA, respectively. The voltage pulse spectrum as a time function in Fig. 5 is just recorded at the critical point (b) ~72 mA of the inseted plot. It is clear that at the beginning, the sweeping trace of the voltage noise spectrum at constant current 72 mA is irregular with a small amplitude, and after several seconds relaxation, the sweeping curve suddenly presents an abrupt voltage drop and simultaneously a series of slow periodic voltage pulse oscillations arises, where the amplitude of the pulses gradually decreases with the increase of the relaxation time and the periodicity remains almost unchanged with an accuracy of 3 sec. Relaxing about 30 min later, the system seems to reach a steady state, where the magnitude of the amplitude of the oscillation approaches a constant value of the order of several millivolts. The value of the periodicity is about 14 sec, i.e., 0.07 Hz. Such a voltage pulse spectrum is measured for the sample used in Fig. 1, but for different quenching times by LN_2, where the sample was played in air for three days and quenched into liquid nitrogen

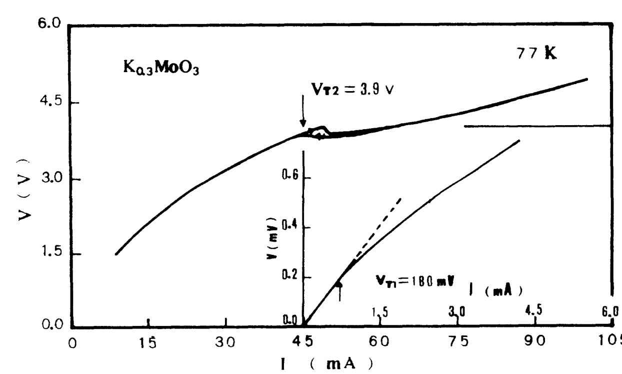

FIG. 4. Typical voltage-current (*V-I*) characteristic with a normal switching for pure blue bronze $K_{0.3}MoO_3$. The inseted plot is the amplified *V-I* curve at low field; the first threshold voltage is about 180 mV.

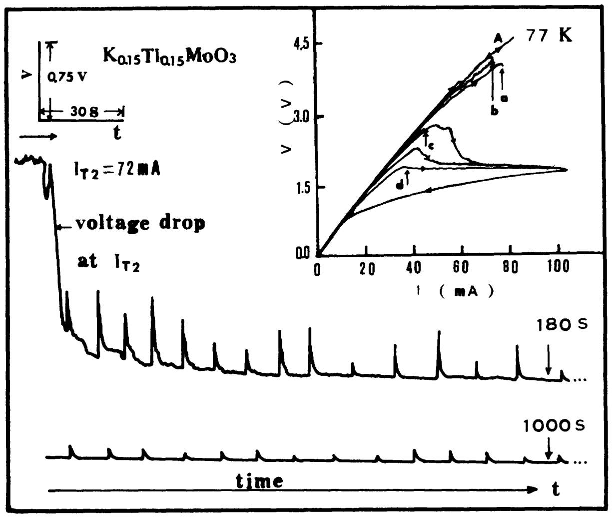

FIG. 5. Low-frequency-voltage-pulse oscillation spectrum recorded by the X-Y recorder as a time function at critical point, $I_{T2} \sim 72$ mA, for $K_{0.15}Tl_{0.15}MoO_3$. The periodicity is about 14 sec. The inseted plot is the corresponding V-I characteristics similar to Fig. 1; (A) is the initial measured curve of the sample quenched by liquid nitrogen without breakdown transition; the arrows labeled (a), (b), and (c) represent the critical point to be taken at the voltage drop. The voltage oscillation spectrum was recorded at point (b). It is seen that the amplitude of the oscillation decreases with the increase of the relaxation time.

again. Figure 6 shows the periodic-voltage pulse oscillation spectra at different critical points 77 and 47 mA, i.e., (a) and (c) points of the inseted plot in Fig. 5. It is seen that for different current cycle times, although the threshold of the breakdown transition is different, the periodicity of the voltage pulse oscillation at different critical points is found to be almost independent on the second threshold current I_{T2} within an accuracy of 3 sec. Such a pulse oscillation can only be observed at the critical point for the quenched impure sample $K_{0.15}Tl_{0.15}MoO_3$.

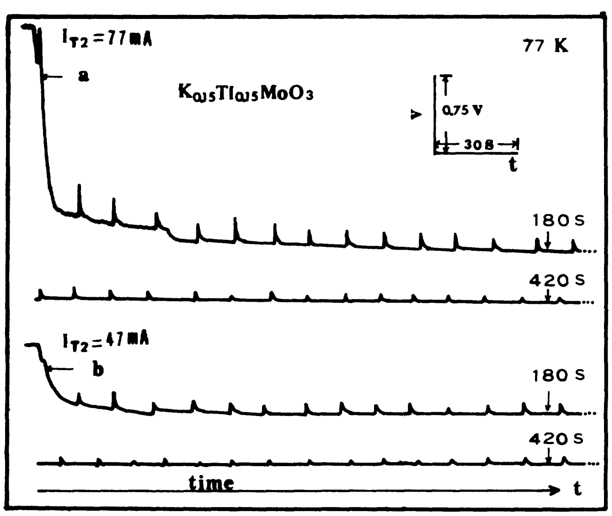

FIG. 6. The periodic voltage pulse oscillation spectra at different critical points 77 and 47 mA.

It is mentioned that such breakdown behavior observed in blue bronzes does not always occur in all samples at 77 K. It seems that this feature is more easily found in the impurity-doped sample than in the pure sample, at least several Tl/W-doped samples investigated have shown this unusually nonlinear transport feature, and the one that we have presented here is the typical one. If such a feature is assumed to result from the heat effect, then a similar phenomenon should be expected in pure samples at 77 K. In fact, the transport properties of the pure samples investigated do not show the similar large voltage drop in high field at 77 K, as well as the large hysteresis similar to that for impurity-doped samples.

IV. DISCUSSIONS

From the overall aspects of the voltage-current characteristics in an impure sample $K_{0.15}Tl_{0.15}MoO_3$, the curves exhibit an extremely large breakdown transition, negative-differential resistance (dV/dI), and the very-low-frequency voltage pulse oscillation at the critical point I_{T2}, as well as a large electronic hysteresis in the nonlinear region. Previously, a similar behavior with complicated hysteresis and low-frequency voltage pulse noise were also found in electron-irradiated[23–25] and W-doped blue bronzes[26] as well as in Fe-doped $NbSe_3$ samples.[27,28] Generally, these phenomena in an incommensurate CDW system were considered to be related to the random distributions of the pinning strengths of the CDW by impurities, contacts, or other lattice defects. The disorder of random pinning leads to the absence of the long-range order of CDW and to the glasslike characteristics of CDW states. The depinning of the CDW condensate under the external electronic field is most probably the cause of the finite threshold for CDW motion and of the strong metastability effects. Although the above model could prove useful for some CDW systems, to our knowledge, up to now the real origins of the similar breakdown phenomena, very-low-frequency voltage pulse, large hysteresis, and zero-differential resistance, are still not clear, and remain controversial. In our case, it is seen that the observed breakdown transition at the critical point with an abrupt voltage drop is unstable for the subsequent current cycle, and the extremely low-frequency voltage pulses and the large hysteresis are clearly the sign of large length scale relaxation, hardly described by the quantum origins of the CDW motions, but quite similar to the mechanical properties of solids. Hence, the observed phenomena might, in detail, need a new theoretical explanation. In this paper, in order to simplify the interpretation of the results, we mainly focus our attention on the Tl-doped sample.

It is interesting that all of the observed features in Fig. 1 have surprising similarities to the stress-strain curve in metallurgy for aluminum alloys[29] where the stress-strain curve often begins smoothly but develops numerous serrations after a sudden plastic deformation. It is also found that these serrations usually occur in freshly quenched commercial Al alloys containing a few percent of allowing solute elements, but do not appear in pure aluminum.[30] This is because the long-scale diffusions of impurities (alloy elements, vacancies, etc.) are responsible for the serrated yielding curves obtained during a tensile deformation. Hence, by comparisons with the CDW system, the CDW condensate with an appropriate superlattice can be viewed as an "electronic crystal," compensated by a positively charged lattice, in which deformations and dislocations can be produced by external forces similarly to the usual crystal solid. These deformations and dislocations will determine the yield point of the electronic crystal, for which an analogous viewpoint was already given by Lee and Rice,[31] Dumas and Feinberg,[32] and Feinberg and Friedel.[33] Although the comparison between *V-I* curves and stress-strain curves in alloys may be not rigorous, the phenomena near the second threshold I_{T2} shown in Fig. 1 can be satisfactorily compared to those occurring at the yield point. The abrupt voltage drop at a second threshold and a negative-differential resistance region above it are very similar to the yield drop in plasticity. A reasonable interpretation can similarly be given in terms of the plastic deformation of the CDW condensate under an applied field, where the greatest deformations and strain in the CDW induced by the external applied field arise at the contacts, perhaps at the impurities' centers of strong pinning and on the roughness of the sample surface.[33-35] Just at the spot the distortions of the CDW lattice will be produced by the field, they can be considered as screwed dislocations, and these dislocations can emit secondary loops under the field.[32,33] Therefore, a possible source of the multiplications or creations of the dislocations is the Frank-Read mechanism, starting from pre-existing dislocation lines, as proposed by Lee and Rice.[31] However, we also note that in our experiment the *V-I* characteristics with breakdown transition do not appear initially for the virgin quenched sample, but only occur under the repeated high conducting current cycles. In addition, the *V-I* curve shows two thresholds: the first is smooth without a voltage drop; the second presents a sudden breakdown transition. Therefore, it might indicate that in the CDW system there may simultaneously exist two kinds of pinning centers, i.e., weak and strong ones. The first threshold corresponds to the depinning of CDW pinned by the weak centers in the presence of the field; in the meanwhile, the other part of the CDW pinned by the strong centers (for example, contacts, etc.) is still strongly localized and cannot move under the high field at several initial measurements. When the samples have undergone several conducting current cycles, the stress of the CDW condensate localized at strong centers will accumulate due to the multiplications of the dislocations and the CDW defects under repeated current cycles. In this way the internal strain and deformations of the CDW condensate localized at the strong pinning centers are growing, when the energy of the localized CDW condensate stored by the repeated external field reaches a finite critical value, a very strong inhomogeneous local electric field in the specimen is generated, and consequently, leads to a breakdown transition at high voltage by the processes of the hot electrons hopping over the localized barriers. In this way, the localized CDW state begins to delocalize and release the accumulated energy, and as a result, leads to the propagation or diffusion of the dislocations and the CDW defects across the CDW crystal with smaller friction with a reduced voltage as the current increases, leading locally to a negative-differential resistance region, also similar to the usual crystal solids above the yield point. When the shearing movement of the CDW as a whole evidently becomes possible, some part of the sample volume, finally, leads to a near-zero-differential resistance.

On the other hand, the very-low-frequency voltage pulse observed at the second threshold point in a quenched impure sample is similar to the serrations in stress-strain curves of Al alloys in the plastic region, where the sudden plastic deformation causes stress relaxation; serrations appear as repeated oscillations of the stress relaxation. Therefore, a similar mechanism can be applied to CDW material where one expects current inhomogeneities localized in filaments, and leads to the voltage fluctuations. The large voltage pulses and the broad band noise appearing at the threshold is, i.e., in our picture, similar to the acoustic emissions reported just above the yield point.[36]

As described in the experimental method above, the unusual properties seem to usually appear on the freshly quenched impure blue bronze, but are not observed in the pure sample. This behavior is also in agreement with that observed in metallurgy, for in the pure Al crystal no serrations appeared in the plastic region.[29] Although we have considered the dislocations and the CDW defects produced by the plastic deformation of the CDW condensate as responsible for strain-aging, it is also possible to retain, temporarily, large numbers of nonequilibrium defects (for example, vacancies, etc.) by quenching from high temperatures. These nonequilibrium defects might interact with the dislocation and speed up the diffusions of the dislocations or the CDW defects, for which the appropriate rate of strain-aging is responsible for the serrations.[29] Though these nonequilibrium defects also exist by quenching in the nominally pure sample, the number of the virgin impurities acted on strong center are relatively smaller than that of impure samples, and, therefore, the rates of diffusion of the dislocations and the CDW defects are far too small to account for the necessary rates of strain aging. This is possibly why in the impure or irradiated samples by quenching we easily observe the low-frequency voltage pulses, breakdown transition at threshold point. In addition, the transit of the breakdown transition from a large voltage drop at the beginning to the final zero-differential resistance state shown in Figs. 1(b) and 1(c) is a slow shift process with a long-scale relaxation. When the current deceases from above, the CDW can be partially pinned again by the strong centers, but these restored processes are not completely reservable for this slow relaxation system due to the permanent plastic deformation of the CDW crystal, and, therefore, the current leads to a large hysteresis. For the subsequent measurement when the current increases again, the barriers of the moving CDW were lowered and this had a smaller threshold. Besides, those nonequilibrium defects might be one of the origins of the slow drift effects with the time seen in Figs. 1, 5, and 6. We also note that such a CDW crystal might be different from the real solids; this is because the CDW crystal, which is plastic deformed or cracked under the tensile force, can almost be restored when the external electric field is released, leading to the behavior in Fig. 2. In contrast to the real solids, once the solid is plastic deformed, the recovery is small. This means that for the CDW system the uniform distribution of the impurities or the CDW defects is not the minimum state of the energy, the pinning state with the nonuniform distribution of the impurities or defects is stable.

In contrast to the above model, Littlewood[37] recently has shown theoretically that at low temperatures in semiconductive compounds with CDW, the nonlinearity dc-voltage characteristics should be bistable. The high-velocity branch, which emerges from the fact that the normal electrons are almost decoupled at high velocities when the CDW moves fairly uniformly, describes free sliding of the CDW. In the low velocity, the CDW is highly deformed, with a velocity low enough that backflow currents of normal carriers can screen the local electric fields produced by the moving CDW. Therefore, a key characteristic of the Littlewood model is that the transition results in a large "S-shaped" bistability in V-I characteristic. A bulk material with an "S-shaped" V-I characteristic is naturally unstable to breakdown to inhomogeneous filamentary conduction. The critical region is a domain of negative-differential resistance and can be observed only in current-controlled measurements. Within the region of negative-differential conductivity the total damping decreases with increasing current. In our measurements, these characteristic behaviors all were observed. Intuitively, our experimental results also seem to be in good agreement with the model of the bistability proposed by Littlewood.[37] However, at present it is difficult to decide which mechanism described here should be attributed to successfully explain the observed surprising results. In addition, whether the final breakdown state of the impure samples can be fundamentally considered as different from the hysteresis behavior seen in the pure sample is still unclear. Hence, a further investigation is needed to clarify.

In conclusion, we have described an unusual nonlinear phenomenon with zero-differential resistance and large hysteresis above the second threshold in Tl-doped blue bronzes, which is accompanied by a low-frequency voltage pulse oscillation and a large voltage drop at I_{T2}. These effects of an electric field on a pinned CDW are phenomenologically interpreted in analogy with the mechanical deformations of alloys. The threshold field is similar to the yield point of a crystal and reflects the appearance of a permanent plastic flow of CDW defects. The repeated current cycling may act as a external-force-induced strain and dislocation loops of the CDW condensate localized at contacts or other strong pinning centers. The onset of plasticity provides a possible explanation for the switching and the very-low-frequency voltage pulse. The origins of the large hysteresis can be attributed to the incompletely reservability of the CDW crystal due to the permanent plastic deformations. In addition, whether these phenomena can also be attributed to the bistable effects of the CDW proposed by Littlewood, still needs to be researched further.

ACKNOWLEDGMENTS

This project was supported by the National Natural Science Foundation of China, and also by the Education Committee of the State Council through the Foundation of Doctoral Training.

[1]A. Wold, W. Kunnman, R. J. Arnortt, and A. Ferretti, Inorg. Chem. **3**, 545 (1964).

[2]J. P. Pouget, S. Kagoshima, C. Schlenker, and J. Marcus, J. Phys. Lett. (Paris) **44**, L113 (1983).

[3]J. Dumas, C. Schlenker, J. Marcus, and R. Buder, Phys. Rev. Lett. **50**, 757 (1983).

[4]For review, see, G. Grüner and A. Zettl, Phys. Rep. **119**, 117 (1985); G. Grüner, Rev. Mod. Phys. **60**, 1129 (1988).

[5]L. F. Schneemeyer, F. J. DiSalvo, S. E. Spengler, and J. V. Waszczak, Phys. Rev. B **30**, 4297 (1984).

[6]R. M. Fleming, L. F. Schneemeyer, and R. J. Cava, Phys. Rev. B **31**, 1181 (1985).

[7]R. J. Cava, P. B. Littlewood, R. M. Fleming, L. F. Schneemeyer, and E. A. Rietman, Phys. Rev. B **41**, 1184 (1986).

[8]R. M. Fleming, R. J. Cava, L. F. Schneemeyer, E. A. Rietman, and R. G. Dunn, Phys. Rev. B **33**, 5450 (1986).

[9]R. M. Fleming, R. J. Cava, and L. F. Schneemeyer, Physica B+C **143**, 95 (1986).

[10]A. Maeda, T. Furuyama, and S. Tanaka, Solid State Commun. **55**, 951 (1985); A. Maeda, T. Furuyama, K. Uchinokura, and S. Tana, *ibid.* **58**, 25 (1986); A. Maeda, M. Notomi, and K. Uchinokura, Phys. Rev. B **42**, 3290 (1990).

[11]L. Mihaly and G. X. Tessema, Phys. Rev. B **33**, 5858 (1986).

[12]G. Mihaly and P. Beauchene, Solid State Commun. **63**, 911 (1987).

[13]G. Mihaly, P. Beauchene, and J. Marcus, Solid State Commun. **66**, 149 (1988).

[14]G. Mihaly, P. Beauchene, T. Chen, L. Mihaly, and G. Grüner, Phys. Rev. B **37**, 6536 (1988).

[15]T. Chen, L. Mihaly, and G. Gruner, Phys. Rev. Lett. **60**, 464 (1988).

[16]S. Martin, R. M. Fleming, and L. F. Schneemeyer, Phys. Rev. B **38**, 5733 (1988).

[17]H. Fröhlich, Proc. R. Soc. London Ser. A **223**, 296 (1954).

[18]R. M. Fleming and L. F. Schneemeyer, Phys. Rev. B **28**, 6996 (1983).

[19]L. Sneddon, Phys. Rev. B **29**, 719 (1984).

[20]P. B. Littlewood, Phys. Rev. B **36**, 3108 (1987).

[21]M. L. Tian, D. C. Tian, Y. Z. Ruan, and R. P. Wang, Solid State Commun. **83**, 171 (1992).

[22]M. L. Tian, D. C. Tian, M. S. Zhang, Q. Chen, and Z. X. Lin, Mod. Phys. Lett. B **6**, 803 (1992).

[23]H. Matka, S. Bouffard, J. Dumas, and C. Schneemeyer, J.

Phys. Lett. (Paris) **45**, L729 (1984).

[24]L. H. Chen, L. F. Schneemeyer, and R. M. Fleming, Phys. Rev. B **29**, 3765 (1984).

[25]S. Bouffard, M. Sanquer, H. Mutka, J. Dumas, and C. Schneemeyer, in *Proceedings of the International Conference on Charge-Density Waves in Solids, Budapest, Hungary, 1984,* edited by Gy. Hutiray and J. Sólyom, Lecture Notes in Solids Vol. 217 (Springer, Berlin, 1985), p. 449.

[26]L. F. Schneemeyer, R. M. Fleming, and S. E. Spengler, Bull. Am. Phys. Soc. **29**, 357 (1984).

[27]Gy. Hutiray, G. Mihaly, and L. Mihaly, Solid State Commun. **47**, 121 (1983).

[28]J. C. Gill, Mol. Cryst. Liq. Cryst. **81**, 73 (1982).

[29]See, for example, A. H. Cottrel, Philos. Mag. **44**, 829 (1953); L. P. Kubin and Y. Estrin, J. Phys. (Paris) **47**, 497 (1986).

[30]A. Berghezan, Rev. Met. **49**, 99 (1952).

[31]P. A. Lee and T. M. Rice, Phys. Rev. B **19**, 3970 (1979).

[32]J. Dumas and D. Feinberg, Europhys. Lett. **2**, 555 (1986).

[33]D. Feinberg and J. Friedel, J. Phys. (Paris) **49**, 485 (1988).

[34]P. D. V. Borodin, S. V. Zaitsev-Zotov, and F. Ya. Nad', Zh. Eksp. Teor. Fiz. **93**, 1394 (1987) [Sov. Phys. JETP **66**, 793 (1987)].

[35]P. J. Yetman and J. C. Gill, Solid State Commun. **62**, 201 (1987).

[36]A. G. Beattie, J. Accoust. Emission **2**, 95 (1983).

[37]P. B. Littlewood, Solid State Commun. **65**, 1347 (1988).